Cover letter

A. Confirmation of author representation

The authors of this work confirm, that this work has not been published before, is not under consideration for publication elsewhere and the publication has been approved by all responsible authors, co-authors and authorities involved.

B. Statement of novelty and significance

The present work is the first time that systematic density and surface tension data of Al-V liquid binary alloys are published. The data collected in this work helps in understanding the liquid Al-V system from both the application and the fundamental point of view. Electromagnetic levitation is used to bypass the difficulties of conventional container-based methods measuring thermophysical properties of liquid and reactive metal melts at high temperatures. Density and surface tension are fundamental thermophysical properties, which are used in many industrial applications, as well as in consecutive research. This work, therefore, provides reliable data and a simple model of density and surface tension for the complete liquid Al-V binary system.

C. Suitable Referees

The following referees are suitable because of their experience in research with electromagnetic levitation as well as thermophysical properties.

1.) Hiroyuki Fukuyama (hiroyuki.fukuyama.b6@tohoku.ac.jp)

2.) Masahito Watanabe (masahito.watanabe@gakushuin.ac.jp)

3.) Andrea Quaini (Andrea.Quaini@cea.fr)

D. Category Preferences

Metals and corrosion

E. ORCIDs

Benedikt Reiplinger: 0000-0002-4247-9991

Jürgen Brillo: 0000-0003-3712-0666

Yusaku Seimiya: 0000-0002-8448-6161

Density and Surface tension of liquid Al, V and their binary alloys measured by electromagnetic levitation

B. Reiplinger[1,*], Y. Seimiya[2], J. Brillo[1]

[1)]Institut für Materialphysik im Weltraum, Deutsches Zentrum für Luft- und Raumfahrt (DLR), 51170 Köln, Germany

[2)] Department of Advanced Materials Science and Engineering, Chiba Institute of Technology, Narashino 275-0016, Japan

[*)] Corresponding author: Benedikt.Reiplinger@dlr.de

Abstract

Both density and surface tension were systematically investigated over a wide temperature and compositional range for the liquid Al-V alloy system. The thermophysical properties were measured in an electromagnetic levitation device. A linear decrease in surface tension and density with increasing temperature was observed for every alloy composition investigated. Additionally, a decrease in density and surface tension was observed for increasing aluminum content among the different probed samples. This decrease is, a strong deviation from an ideal mixing behavior which was experienced for both properties. Different models, including variants of the well-established Butler model, were employed to better describe the compositional dependence of density and surface tension in the liquid Al-V system. The advantages and disadvantages were discussed for each model describing the measured thermophysical property data. Strong similarities were observed when comparing the mixing behavior and segregation effects of the investigated Al-V system with already established works for the liquid Al-Ti system. The results suggest that both vanadium and titanium show similar mixing behavior when paired with aluminum.

Keywords: Electromagnetic Levitation, liquid aluminum, liquid vanadium, surface tension, thermophysical properties

I. Introduction

A. Motivation

Aluminum [1] and vanadium [2] are the two most common alloying elements for titanium-based alloys used in high performance applications, such as the aerospace [3] or biomechanical industry [4]. Both elements are used to improve the high specific strength [4], excellent heat [5, 6] and corrosion resistivity [7], while simultaneously providing a low density and superior biocompatibility [8] of titanium alloys. Ti-6Al-4V, the most commonly used titanium-based alloy [9], combines both alloying elements for excellent physical and mechanical properties in a wide variety of applications.

Even though the Al-Ti-V system is highly relevant both industrially and scientifically, there is rarely any research that covers the complete alloy system. It is the goal of our work to provide fundamental thermophysical property data, as well as profound scientific insight for the entire Al-Ti-V system. Our course of action is to start by investigating the binary sub-systems Al-Ti, Al-V and Ti-V and subsequently work our way up to the complete ternary system. Our previous works focused on the thermophysical properties, e.g. density, molar volume and surface tension, of the Al-Ti [10, 11, 12] and Ti-V [13, 14] system. In this work we expand our research, onto the Al-V system.

Thermophysical properties are tremendously interesting from an industrial and a scientific standpoint. In the industrial environment, thermophysical property data such as density or surface tension is regularly used as optimization parameters during process design. Alloys from the Al-Ti-V system are used in variety of manufacturing processes, ranging from traditional casting [15, 16] to the more recent additive manufacturing [17, 18, 19]. The design and optimization for these processes heavily rely on precise knowledge of the thermophysical properties of the manufactured alloy.

Therefore, this work serves two goals: Firstly, we want to provide reliable, reproducible data on density, molar volume and surface tension for the binary Al-V alloy system. Secondly, we want to develop reliable models that consistently reproduce the experimentally determined data. These models subsequently help us in gaining further fundamental insight in the mixing behavior of the Al-V system.

In order to achieve these goals, we need to apply an experimental method that allows us to process the highly reactive alloy system Al-V at very high temperatures (up to 2300K), without the risk of contamination. With the containerless electromagnetic levitation (EML) technique many of the difficulties accompanying the investigation can be handled. EML has been applied to thermophysical property measurements by many previous works [20, 21] and shows numerous beneficial qualities, such as accessible high temperatures, high undercooling and the possibility to process highly reactive melts when compared to traditional container-based measurement methods [20].

B. Density and excess volume

The density of most liquid metals within a finite temperature range including the melting temperature can be expressed as [22]:

$$\rho(T) = \rho_L + \rho_T(T - T_L) \tag{1}$$

With T_L being the liquidus temperature, ρ_L, the density at the liquidus temperature and, ρ_T, the density temperature coefficient. As the density is defined as the mass over the volume, the density of a mixture of *N* pure components $0 < i < N$ can be written as:

$$\rho = \frac{\sum_i x_i M_i}{\sum_i x_i V_i + V^E} \tag{2}$$

Thereby, x_i is the mole fraction of the component *i* while M_i is the corresponding molar mass. The molar volume of the mixture is described by the denominator in Eq. (2), as the sum of the molar volume V_i of every pure component and the molar excess volume V^E. For an ideal solution the excess volume equals zero, reducing the molar volume of the mixture to a linear combination of molar volumes of the pure elements. Analogously to the excess free energy, a Redlich-Kister form can be used to express V^E. For a binary system this reads as:

$$V^E = x_i(1 - x_i) \sum_{\upsilon=0} {}^{\upsilon}V(T)(x_i - (1 - x_i))^{\upsilon} \tag{3}$$

Here, ${}^{\upsilon}V(T)$ denotes the linearly temperature dependent interaction coefficient of order ν between the components. For most cases the first constituent $\upsilon = 0$ is sufficient to approximate the excess volume for a regular solution of two elements. We will show, that in the case of Al-V the excess molar volume can be approximated simply by a parabola:

$$V^E_{Al,V} \approx x_{Al} x_V \; {}^{0}V(T) \tag{4}$$

C. Surface Tension

Just like the density, the surface tension γ can be described over a reasonably small temperature interval as a linear function of *T*:

$$\gamma(T) = \gamma_L + \gamma_T(T - T_L) \tag{5}$$

In Eq. 5, T_L is the liquidus temperature, γ_L is the surface tension at the liquidus temperature and γ_T is the temperature coefficient.

D. Renovated Butler model

Kaptay [23] deduced from the thermodynamic definition of the surface tension, $\gamma = \left(\frac{dG}{dA}\right)_{p,T,n_i}$, with *G* being the total free energy of the system and *A* the total surface area that, in a multicomponent liquid solution with *N* components, the following relation is valid:

$$\gamma = \gamma_i = \gamma_j = \ldots = \gamma_N \tag{6}$$

The previous expression is called Renovated Butler equation and γ_i is called "partial surface tension" of component *i*. In Eq. (6), the γ_i's have to be calculated according to the following expression:

$$\gamma_i = \gamma_i^0 \frac{\omega_i^0}{\omega_i} + \frac{RT}{\omega_i} ln\left(\frac{a_i^S}{a_i^B}\right) \tag{7}$$

where γ_i^0 is the surface tension of component *i* in pure liquid *i*. Analogously, ω_i^0 is the molar surface area of component *i* in pure liquid *i* and ω_i is the partial molar surface area of component *i* in the solution. Kaptay [23] derived equations 6 and 7 from the fundamental Gibbs thermodynamics by introducing a new property, namely the partial surface area. No assumptions about the structure of the surface or the bulk need to be made. Together Eqs. (6) and (7) form the Renovated Butler model. The partial molar surface area is related to the molar surface area and the molar excess volume,

$$\omega_i = \omega_i^0 + (x_j^S)^2 L_\omega \tag{8}$$

where the parameter L_ω abbreviates the term related to ${}^0V$ in Eq. (4):

$$L_\omega = N_{Av}^{\frac{1}{3}} ({}^0V)^{2/3} \tag{9}$$

Here, N_{Av} is the Avogadro number. By introducing the partial molar excess free energies for both, bulk ${}^E g_i^B(T, x_i^B)$ and surface ${}^E g_i^S(T, x_i^S)$, equation 7 becomes the following expression:

$$\gamma_i = \gamma_i^0 \frac{\omega_i^0}{\omega_i} + \frac{RT}{\omega_i} ln\left(\frac{x_i^S}{x_i^B}\right) + \frac{1}{\omega_i} ({}^E g_i^S(T, x_i^S) - {}^E g_i^B(T, x_i^B)) \tag{10}$$

Eq. 10 is often used for practical calculations. In order to use this equation, models for both the bulk and surface partial molar excess Gibbs energies need to be implemented. For the bulk phase the integral excess free energy can be calculated following a Redlich-Kister polynomial. In the Al-V binary system this reads:

$${}^E g^B(T, x_{Al}^B, x_V^B) = x_{Al}^B x_V^B \sum_v {}^v L_{Al,V}(T) \cdot (x_{Al}^B - x_V^B)^v \tag{11}$$

The corresponding parameters ${}^v L_{Al,V}(T)$ can be found in thermodynamic assessments such as Ref. [24]. In this work the summation was ended after the second constituent $v = 1$. In most cases, the excess free energy for the surface phase is modelled using the same functional relationship as used for the bulk

phase but as a function of the surface composition x_i^S, instead of the bulk composition x_i^B. It needs to be mentioned, that the calculations can vary, depending on which Redlich-Kister parameters are used.

E. Conventional Butler model

The Renovated Butler Equation [25] contains the Conventional Butler equation as a limiting case.

The Conventional Butler model was derived using the assumption that the surface forms a separate phase in equilibrium with the bulk phase. Surface and bulk have individual compositions and a chemical potential can be assigned to each of them. The chemical potential of the surface has a contribution from the surface tension and the remaining part has the same functional form of that of the bulk, except that it applies to the surface composition and there is also a factor $0 < \beta \leq 1$ which relates the coordination in the surface to that in the bulk [26]. Thus, the factor requires some assumptions about the surface structure and different values were favoured for it in the past.

For the binary Al-V system, the Conventional Butler equation may be written as follows:

$$\gamma = \gamma_{Al}^0 + \frac{RT}{\omega_{Al}^0} ln\left(\frac{a_{Al}^S}{a_{Al}^B}\right) = \gamma_V^0 + \frac{RT}{\omega_V^0} ln\left(\frac{a_V^S}{a_V^B}\right) \tag{12}$$

It can easily be seen, that Eq. (12) follows directly from Eq. (7) of the Renovated Butler model when the partial molar surface areas can be approximated by the surface areas of the pure components, i.e. when $\omega_i \approx \omega_i^0$. According to Eq. (8), this is usually the case, when the molar excess volume is very small. For an ideal solution with zero molar excess volume, the Conventional Butler model and the renovated one are even identical. Analogously to Eq. (10), Eq. (12) may be written as

$$\gamma = \gamma_{Al}^0 + \frac{RT}{\omega_{Al}^0} ln\left(\frac{x_{Al}^S}{x_{Al}^B}\right) + \frac{1}{\omega_{Al}^0}\left({}^E g_{Al}^S(T, x_i^S) - {}^E g_{Al}^B(T, x_i^B)\right) \tag{13}$$

so that excess free energies from data-bases can be used.

As described earlier, the partial molar free energies of the surface have the same mathematical form as those of the bulk, with an additional factor β that accounts for the different coordination in the surface and in the bulk. With $\beta = 0.83$ in agreement with Ref. [25] the partial molar free energies yield:

$${}^E g_i^S(T, x_i^S, ..) = \beta\, {}^E g_i^B(T, x_i^S, ..) \tag{14}$$

In the case of an ideal solution, the excess free energy equals zero. When it is further assumed that all areas are equal, i.e $\omega_i^0 = \omega_j^0 \equiv \omega$, Eq. (13) can be written for the binary system Al-V as:

$$\gamma = \gamma_{Al}^0 + \frac{RT}{\omega} ln\left(\frac{x_{Al}^S}{x_{Al}^B}\right) = \gamma_V^0 + \frac{RT}{\omega} ln\left(\frac{1 - x_{Al}^S}{1 - x_{Al}^B}\right) \tag{15}$$

Eq. (15) can be solved analytically for x_{Al}^S:

$$x_{Al}^S = \frac{x_{Al}^B}{x_{Al}^B + (1 - x_{Al}^B) S_e(T)} \tag{16}$$

With the segregation factor $S_e = \exp((\gamma_A - \gamma_B)\omega/RT)$.

F. Egry model

Egry [27] adapted the ideal solution approach introduced with the Conventional Butler model in Eq. 15 for compound forming systems. He assumed that the compounds formed in a liquid binary alloy do not segregate to the surface and, therefore, do not contribute to the surface tension of the liquid. This assumption alters the segregation factor $S_e(T)$ by a factor of $f_{Se} * (n+m)(x_A^B)^n(x_B^B)^m$, accounting for the energy contribution by an A_nB_m compound not segregating to the surface. Subsequently, S_e reads:

$$S_e(T) = \exp\left(\frac{(\gamma_A-\gamma_B)\omega - f_{Se}*(n+m)(x_A^B)^n(x_B^B)^m}{RT}\right) \quad (17)$$

with f_{Se} being an adjustable parameter related to the single bond energy in the compound. For this model, ω was also fitted.

With the similarities in formalisms, one can easily see the common origin of all three of these models introduced to describe the surface tension for a binary liquid alloy. Yet, each approach implements different assumptions. Therefore, all three methods will be reviewed against each other and against the background of the measurements made in this work.

II. Experimental

A. Sample Processing

All measured samples were prepared from high purity vanadium (99.995 pct., supplied by smart elements) and aluminum (99.999 pct., supplied by alfa Aesar). After weighting in the appropriate amount of both elements for every corresponding composition, the metals were cleaned in an ultrasonic bath. Afterwards, the samples were pre-alloyed in an arc furnace under a protective argon (99.9999 vol pct. purity) atmosphere, resulting in droplet-like samples with diameters in the range of 5-7mm. Since levitation and heating behavior varies with both sample material and size, the sample diameter was adjusted to achieve optimal levitation and heating for every composition. Finally, the samples underwent another cleaning cycle in the ultrasonic bath right before the experiment.

The levitation apparatus consists of a water-cooled copper coil inside a vacuum chamber. The chamber with the sample already being installed was evacuated for cleaning purposes to a base pressure of 10^{-8} mbar. The actual experiments were carried out afterwards under protecting gas atmosphere consisting of high purity (6N) Ar, He, or a mixture of both.

At the experiment start, the sample rests on an alumina specimen holder inside the copper coil. Applying a current of about 200A with a frequency of 250 kHz to the coil, generates an alternating, inhomogeneous electromagnetic field. This alternating field induces eddy currents inside the metallic sample, subsequently heating the sample via ohmic losses and simultaneously levitating the sample through Lorenz forces. Therefore, heating and positioning of the sample are not decoupled and a cooling gas must be applied to control the sample temperature. The cooling gas, which is identical to the gas atmosphere is applied through the alumina specimen holder in a laminar flow. A more detailed description of the electromagnetic furnace used in this work can be found in references [20, 22, 28].

During the levitation process, the sample temperature is monitored using a single-color pyrometer (1.45 µm - 1.8 µm wavelength). The precise emissivity of the sample, which strongly varies with composition, is generally unknown. Therefore, a temperature correction is needed to determine the true temperature of the sample. The following temperature correction, was introduced in many previous works using the EML technique [22, 28, 29]:

$$\frac{1}{T} - \frac{1}{T_P} = \frac{1}{T_L} - \frac{1}{T_{L,P}} \qquad (18)$$

With this correction, the true sample temperature T, can be determined using the pyrometer signal T_P, the true liquidus temperature T_L, as well as the liquidus temperature observed with the pyrometer $T_{L,P}$. The true liquidus temperature is taken from Reference [30], while $T_{L,P}$ is observed as a disruption in the pyrometer signal.

B. Density Measurement

The optical dilatometry method [20, 31] is used to determine the density of a levitating sample. Thereby, an expanded laser is employed to capture a shadowgraph image of the sample with a CCD camera chip. Several optical elements ensure that only direct laser light reaches the camera. Around 2500 of these images are taken for a single measurement. The edge curve radius, is detected with an algorithm for every frame. The pixel volume V_P can be calculated from the edge curve radius. From the sample volume in pixels, the real sample volume can be derived. Therefore, a calibration with metal balls of precisely known volume is done (RB-4.762/GW20 DIN 5401). The sample mass is measured

before and after the experiment using a high precision scale, to ensure that no significant mass loss, due to potential evaporation, occurs. A more detailed explanation on the density measurement can be found in previous works [22, 28, 32].

A very detailed error estimation for the density measurements using EML and the optical dilatometry method used in this work can be found in [32]. The main error sources are: mass loss, calibration or temperature error, strong sample movement and a distorted sample shape and symmetry. The usual total error can be calculated using the formula below and lays around $\pm 1\%$.

$$\frac{\Delta\rho^2}{\rho^2} = \frac{\Delta m^2}{m^2} + \frac{\Delta q^2}{q} + \frac{\Delta V_p^2}{V_p^2} + \left(\frac{\partial V_p}{\partial T}\right)^2 \frac{\Delta T^2}{V_p^2} \qquad (19)$$

C. Surface Tension Measurement

The oscillating drop method is a well-established method to determine the surface tension of levitating droplets. It has been explained in great detail in numerous previous works [33, 34, 35, 36, 37]. The general concept of this method is to record the frequency of the surface oscillation of an excited liquid metal droplet and correlate the surface tension to the so observed frequency. The Rayleigh equation correlates the frequency, ω_R, of such a surface oscillation with the surface tension, γ, for a spherical, non-rotating droplet of a known mass, m_S. This correlation is only valid for a force free, spherical droplet. The Rayleigh mode is five-fold degenerate. However, under terrestrial conditions, the sample is neither force free nor spherical and the 5-fold degeneracy to the $l = 2$ mode is lifted. If, in addition, there is also slight rotation around the vertical axis, five distinct frequencies $\omega_{2,m}$ ($-2 \leq m \leq +2$) become visible for the surface oscillation of the sample.

The frequencies $\omega_{2,m}$ can be used to calculate the surface tension γ of a molten metal droplet, following the sum rule of Blackburn and Cummings [38]:

$$\gamma = \frac{3m_S}{160\pi}\left(\sum_{m=-2}^{2} \omega_{2,m}^2 - 9.5\Omega^2 - 1.5\left(\frac{g}{a}\right)^2 \Omega^{-2}\right) \qquad (20)$$

In Eq. (22), g = 9.81 g·m^{-2} is the gravitational constant, a is the radius of the sample with approximated spherical shape and $\Omega^2 = 1/3(\omega^2_X + \omega^2_Y + \omega^2_Z)$ is a correctional parameter accounting for the magnetic pressure the sample experiences due to electromagnetic levitation. It is calculated from the translational frequencies, $\omega_{X,Y,Z}$, of the sample in horizontal (x-, y-) and vertical (z-) direction. A more in-depth description, on how the surface tension is determined from a recorded oscillation spectrum can be found in [22].

A detailed error approximation can be found in [32]. The surface tension measurement underlies the same error sources associated with positioning and heating during levitation as the density measurement. Additional error sources are introduced with the new measured variables. The surface tension measurement carried out in this work has an average error of $\pm 5\%$.

III. Results

A. Density

The density was measured for ten different alloys in the Al-V system, including the pure elements Al and V. The composition of each investigated alloy, as well as the corresponding liquidus temperature, taken from [30], can be found in Table 1. The $Al_{30}V_{70}$ composition could not be measured due to extreme evaporation of the sample during processing. For all other compositions a reasonable measurement could be carried out over a temperature range of at least 200 K. The density was measured during incremental cooling with a laminar gas flow. After each temperature step, the sample was given 60 seconds to reach an equilibrium. The corresponding densities versus temperature for each alloy are plotted in Fig. 1. As expected, for all samples a linear decline in density can be observed with increasing temperature. The density could be measured between 900K and 2250K, depending on the alloy composition. The maximal achievable temperature for each individual measurement increased with increasing vanadium content. Density values between $2.12\ \mathrm{g\ cm^{-3}}$ (for pure aluminum) and $5.58\ \mathrm{g\ cm^{-3}}$ (for pure vanadium) were observed. As expected, the density for all binary alloys varies between that of pure aluminum and pure vanadium. An increase in density can be observed with an increase in vanadium content. The experimental scatter increases towards a composition of 50% Al and 50% V. This can be largely attributed to a stronger sample movement of samples with a higher alloying content.

All measured samples allow for a linear fit following equation 1. The corresponding ρ_L and ρ_T values are listed in table 1 together with the melting temperature T_L and the density at 1973K. Table 2 compares the gathered parameters for the pure elements with already existing literature data for pure Al and V [39, 40]. The findings are in good agreement with both our own previous work and different already existing literature.

B. Surface Tension

The surface tension was investigated analogous to the density. All compositions were investigated during step-wise cooling with a laminar gas flow. After each step a 60s isothermal hold was performed to allow the sample to equilibrate. The surface tension could be measured between 1000K and 2300K, with the minimum and maximum temperature of each individual measurement increasing with increasing vanadium content. Each measurement could be carried out over at least 200K. The resulting surface tensions are plotted against the temperature in Fig. 2. Aluminum exhibits the smallest surface tension at the liquidus temperature with $0.724\ N\mathrm{m^{-1}}$, while vanadium has the highest surface tension at the corresponding liquidus temperature with $2.069\ N\mathrm{m^{-1}}$. The surface tension for all investigated alloys ranges between those of the pure elements in accordance with the sample composition.

All measurements allowed for a linear fit following equation 5, all of which are included in Fig. 2. Table 3 gives an overview over all processed compositions as well as the respective liquidus temperatures T_L, fitting parameters γ_L and γ_T and the surface tension $\gamma(1800K)$ at 1800K. The measured surface tension for the pure elements lies within good agreement of both our own previous works and available literature data. Table 4 shows a comparison of the surface tension at 1800K and the corresponding fitting parameters γ_L and γ_T for our work and different literature results.

IV. Discussion

A. Density

To investigate the compositional dependence of the density for the Al-V system linear fits from Fig. 1 were used. From the linear fits, the densities are calculated at a reference temperature of 1800K. The reference temperature was chosen, because it lies in the middle between the highest and lowest measured temperature. The resulting plot of the density versus the mole fraction of aluminum at 1800K is shown in Fig. 3. The density decreases nearly linearly from 5.65 g cm^{-3} for pure vanadium to 2.14 g cm^{-3} for pure aluminum. The calculated density for an ideal solution of Al-V ($V^E = 0$), as well as a calculated fit for a regular solution ($V^E_{Al,V} \approx x_{Al}x_V\ {}^0V(T) \approx -5.55\ cm^3mol^{-1} \cdot x_{Al}x_V$), both according to Eq. 2, are also included.

Additionally, Fig. 4 shows the molar volume versus the mole fraction of aluminum for the Al-V system. The measured molar volume increases convexly with increasing aluminum content from 9.02 cm^3/mol to 12.64 cm^3/mol below the ideal molar volume, showing the expected oppositional trend compared with the density. Fits for the ideal and regular solution, following the denominator in Eq. 2 are included as dashed (ideal) and solid (regular) lines. The system does not follow the linear trend of the ideal solution, but follows the fit calculated for the regular solution.

The non-ideality of the system becomes even more evident when one takes a look at the excess volume plotted against the bulk mole fraction of aluminum, as done for 1800K in Fig. 5. The excess volume can be described by the binary interaction parameter, ${}^0V(T)$, introduced in Eq. 4. For the Al-V system a fit following equation 4 yields ${}^0V = -5.55\ \mathrm{cm^3mol^{-1}}$. These findings compares well with the interaction parameters experimentally observed for other Al-alloys. Previous works have shown parameters of $-5.0\ \mathrm{cm^3mol^{-1}}$ for Al-Ni [41], $-3.37\ \mathrm{cm^3mol^{-1}}$ for Al-Cu [42] and $-2.68\ \mathrm{cm^3mol^{-1}}$ for Al-Ag [42]. Additionally, the excess volume is negative, as is often observed in Al alloys containing transition metals [22]. Therefore, the liquid Al-V fits very well into the group of alloy systems showing strong attractive interactions which many Al-based alloys fall into [22].

The temperature dependence of the density can be examined in more detail, when plotting the temperature coefficient, ρ_T, versus the aluminum concentration x^B_{Al}, as done in Fig. 6. A minimum in the temperature coefficient can be obtained around 50% aluminum. If the temperature dependence of the excess volume is neglected, the temperature coefficient can be calculated as follows:

$$\rho_T = \frac{\sum_i x_i M_i * \sum_i x_i \frac{M_i \rho_{T,i}}{\rho_i^2}}{(V^{id} + V^E)^2} \qquad (21)$$

The excess volume can be calculated using the fit introduced in Eq. 4. Figure 6 shows two calculations, one for the ideal solution, where $V^E = 0$, and one for the regular solution, where V^E was calculated according to Eq. 4. Again, the non-ideality of the system can be observed. It should also be noted that if the excess volume is known, the temperature coefficient, which is closely linked to the thermal expansion coefficient, can be calculated solely from properties of the pure elements.

In our previous works [13] we have carved out a similar mixing behavior of titanium and vanadium based upon their ideal mixing behavior. It is highly interesting to compare the findings for the Al-V systems in this work with previous investigation on the Al-Ti system since we expect similar mixing behavior for both elements when alloyed with aluminum. Moreover, our long-term goal is to investigate the ternary Al-Ti-V system. Figure 7 compares the excess volume of the liquid Al-V system

with the excess volume of the liquid Al-Ti system at 1800K. It is easy to see that both systems show a similar mixing trend. Especially for low alloying compositions, close to the pure elements, both curves are almost identically. It has to be considered that for the calculations done the Al-Ti system higher terms than just ${}^{0}V$ must be used for the fitting of the excess volume. Therefore, slight differences in the fitting curve are expected. Nonetheless, the findings strengthen our assumption that titanium and vanadium have analogous mixing behavior.

When integrating the mixing behavior of Al-V with regards to the excess volume, into already existing classifications the similarities between vanadium and titanium are further highlighted. Brillo et. al. [22, 43] connected the excess volume of several binary systems with their respective excess free energy. Just like the Al-Ti system, Al-V falls into the class of alloys that show strong attractive interactions, i.e., alloys that display a strongly negative excess volume.

B. Surface Tension

To investigate the compositional dependence of the surface tension for the Al-V system, the linear fits (Fig.2 and table 3 respectively) were to determine the surface tension for each alloy at the reference temperature of 1800K. The results are shown in Fig. 8 which includes several calculations using different models to predict the surface tension depending on the bulk molar fraction of aluminum. As expected, the measured surface tension decreases with increasing aluminum content from 2.069 Nm^{-1} for pure vanadium to 0.723 Nm^{-1} for pure aluminum.

The mathematically most basic model introduced earlier is the Conventional Butler model applied for the ideal solution. Using this model, the surface tension can be estimated for any bulk composition, according to Eq. 15, when knowing the surface tension of one pure element and assuming the partial surface area for the same component. These calculations are represented by the dashed line in Fig. 8 and are labeled as ‘Conventional Butler ideal’. Considering the observations for the density measurements, it is not surprising that the measured data is not well reproduced qualitatively or quantitatively. Just as for the density, the surface tension data is underestimated when assuming an ideal solution. Therefore, one can assume that the Al-V system is non-ideal with regards to the surface tension.

Since the system does not behave like an ideal solution, the next logical step is to include excess free energies in the calculations introduced above. The resulting calculations, corresponding to Eq. 13, are included in Fig. 8 as a dotted line and are labeled as ‘Conventional Butler non-ideal’. The data is now way better represented. The Redlich-Kister parameters used for Eq. 13, were taken from Ref. [44] and are listed in table 5. The Conventional Butler model for the non-ideal case predicts values very close to the measured surface tension for aluminum mole fractions smaller than 0.2 and larger than 0.8. Between those mole fractions, the surface tension predicted is below the measured data. For the sake of clarity, only the most recent assessment was used.

The next model evaluated against the measured data is the Renovated Butler model introduced by Kaptay [25]. The calculations for this model are done using Eq. 10. Fig. 8 shows these as a solid line. For the Renovated Butler model, the ideal solution was not taken into consideration, since it was shown earlier, that the system does not behave like an ideal solution in regards to the surface tension. Therefore, all calculations labeled ‘Renovated Butler’, refer to the non-ideal case. The Renovated Butler model predicts the data better for alloy compositions between 0.2 and 0.8 while still being reasonably accurate for high aluminum and vanadium mole fractions respectively.

The last model included in Fig. 8 is the Egry model discussed in Sec. I. The segregation factor was calculated using Eq. 16 assuming *n* and *m*, for AlV_3 as the main forming species. The results are represented by the dashed-dotted line. A better agreement with the measured data can be obtained for

alloy compositions between 0.2 and 0.8, then for the Conventional Butler and Renovated Butler model respectively. A slight deterioration for the edges (pure elements) is observed.

When trying to justify the differences in reproduction quality by looking at the formalisms of the different models it becomes apparent, that the main differences for these prediction models is a combination of the surface area for the different species as well as the calculated excess quantities. Regarding the excess quantities, the possibility that the thermodynamic assessments consulted for the Redlich-Kister parameters might not be perfectly accurate, has to be considered. This is supported by the many older parameter sets that can be found for Al-V in the literature.

Similar to the temperature dependence for the density, the temperature dependence of the surface tension can be analyzed in more detail when looking at the temperature coefficient γ_T of the surface tension. Fig. 9 shows γ_T versus the aluminum content. As for the density, the edges of the compositional range, closer to the pure elements, show a lower temperature dependence of the surface tension. For a composition of 30 at.-% aluminum, a maximum in temperature dependence, can be observed. The measured data can be compared to the values predicted by the Conventional Butler model for the ideal solution and the Renovated Butler model for the regular solution. Therefore, the surface tension, γ, at 1790K and 1800K is calculated and subsequently the temperature coefficient can be obtained as $\gamma_T = (\gamma(1810K) - \gamma(1790K))/20K$. The temperature coefficient predicted for the ideal solution, following the Conventional Butler model (Eq. 15) greatly overestimates the values, even showing a different trend to the measured data, for aluminum mole fractions lower than 0.5. The prediction for the regular solution, according to the Renovated Butler model (Eq. 10), reproduces the general trend way better. The regular solution calculations also reproduce the maximal temperature dependence for an aluminum mole fraction of around 0.25.

Moreover, the surface tension behavior can also be used to gain some insight into the compositional behavior of the liquid metals surface. Fig. 10 shows the aluminum content of the surface x_{Al}^{S} in dependence of the bulk aluminum mole fraction x_{Al}^{B}, calculated for the Conventional Butler model for the ideal (dashed) and regular (dotted) solution as well as the Egry model (solid). All curves deviate from a linear trend. This behavior is caused by the segregation effect. Since surface tension can be viewed as a free energy per area [22], one can expect that an alloy system tends to minimize its free energy per surface by depleting the surface layer of the element with the higher surface tension. In the Al-V system, vanadium has the higher surface tension, hence a strong depletion of vanadium in the surface layer is expected as predicted by the Conventional Butler model (dashed line) for an ideal solution. Since our system does not behave like an ideal solution, but instead exhibits attractive interactions (${}^{E}g < 0$), a much less prominent segregation effect, as predicted by the regular solution model (e.g. the Egry model), can be anticipated. Nonetheless, all models predict a depletion in vanadium and an enrichment in aluminum for the Al-V system.

The segregation is a great aspect to utilize when comparing the Al-V system with the Al-Ti system. Earlier in this work (see IV. A) a similar mixing behavior was assumed for Ti and V. When comparing the segregation for both elements mixed with aluminum, this assumption can easily be verified. As shown in Fig. 11 the segregation behavior of V and Ti when mixed with aluminum is very similar. For an ideal solution a very strong depletion of V and a slightly lower depletion of Ti is predicted when mixing with aluminum. This depletion is significantly weakened when assuming a regular solution with Al. The aluminum surface mole fraction predicted with the Conventional Butler model for the regular solution is almost identical for V and Ti. The different temperatures, at which the calculations have been carried out need to be considered. The calculations for the Al-Ti system have been taken from Ref. [10].

V. Conclusion

Density and surface tension have been measured for the liquid Al-V system over a large temperature range and the complete compositional range. Both density and surface tension decrease linearly with temperature for all investigated alloy compositions. Therefore, reference values for the density and surface tension at the liquidus temperature, as well as the corresponding temperature coefficients are given. The compositional dependence was investigated for both properties at a fixed reference temperature. Different models have been deployed to predict the experimentally measured data from the composition. The present work shows that for density and surface tension the Al-V system mixes highly non-ideal. For the density the experimental data could be well reproduced by the model for a regular solution. For the surface tension different models predict the experimental values better in different compositional areas. Regarding the surface tension, a great deal of attention has to be paid to the surface areas and excess quantities used when employing different models. The findings of this work suggest a slight inaccuracy in the Redlich-Kister parameters used for the model calculation applied.

The segregation behavior has been used to compare the Al-V system with the Al-Ti system. The similar mixing behavior of Ti and V proposed by earlier works [14, 13], could be confirmed for the mixing with Al. Both Ti and V show almost identical behavior when mixing with aluminum. This expertise could be an exceptional starting point for a more detailed investigation of the ternary Al-Ti-V system. It is highly interesting to see if how far-reaching this exchangeability between Ti and V goes when regarding the ternary system.

Tables

Table 1: Parameters T_L, ρ_L, ρ_T and $\rho(1800\ K)$ for the density measurements carried out in the Al-V system

Composition	T_L[K]	ρ_L[g cm^{-3}]	ρ_T[10^{-4}g cm^{-3}K^{-1}]	$\rho(1800\ K)$[g cm^{-3}]
V	2183	5.51±0.15	-3.56±0.07	5.586
$V_{90}Al_{10}$	2130.5	5.26±0.17	-4.08±1.28	5.325
$V_{80}Al_{20}$	2108	4.90±0.40	-3.99±0.44	4.953
$V_{60}Al_{40}$	2090.5	4.54±0.29	-5.27±1.15	4.387
$V_{50}Al_{50}$	2055.5	4.09±0.17	-4.58±1.07	4.010
$V_{40}Al_{60}$	1930.5	3.83±0.17	-4.95±1.38	3.422
$V_{30}Al_{70}$	1803	3.67±0.11	-3.70±0.52	3.125
$V_{20}Al_{80}$	1580.5	2.96±0.15	-4.61±0.57	2.782
$V_{10}Al_{90}$	1485.5	2.56±0.11	-2.91±0.41	2.419
Al	933.45	2.33±0.12	-2.15±0.88	2.099

Table 2: Parameters T_L, ρ_L, ρ_T and $\rho(1800\ K)$ obtained for the pure elements Al and V in this work compared to literature data obtained using different measurement techniques. The method abbreviations are: EML = electromagnetic levitation, L = Literature Review, SD = sessile drop, ESL = electrostatic levitation.

Composition	ρ_L[g cm^{-3}]	ρ_T[10^{-4}g cm^{-3}K^{-1}]	$\rho(1800\ K)$[g cm^{-3}]	Reference	Method
Al	2.33±0.12	-2.15±0.88	2.09	This work	EML
Al	2.30±0.02	-2.18±0.32	2.09	[10]	EML
Al	2.36±0.03	-3.30±0.03	2.02	[42]	EML
Al	2.37±0.015	-3.11±0.2	2.05	[45]	L
Al	2.37	-2.6	2.10	[39]	SD
V	5.51±0.15	-3.56±0.07	5.59	This work	EML
V	6.0±0.08	-3.2	6.06	[40]	EML
V	5.46±0.1	-4.9	5.56	[46]	ESL
V	5.36	-3.2	5.43	[47]	L

Table 3: Parameters T_L,γ_L, γ_T and $\gamma(1800\ K)$ for all compositions measured in the Al-V system.

Composition	T_L[K]	$\gamma_L[\mathrm{Nm}^{-1}]$	$\gamma_T[10^{-4}\mathrm{Nm}^{-1}K^{-1}]$	$\gamma(1800\ K)[\mathrm{Nm}^{-1}]$
V	2183	1.935±0.07	-3.51±0.66	2.069
$V_{90}Al_{10}$	2162	1.572±0.09	-5.789±0.75	1.781
$V_{80}Al_{20}$	2138	1.468±0.09	-6.772±0.88	1.696
$V_{70}Al_{30}$	2107	1.245±0.08	-7.651±1.00	1.479
$V_{60}Al_{40}$	2045	1.214±0.07	-7.186±0.93	1.390
$V_{50}Al_{50}$	1949	1.219±0.08	-5.656±0.74	1.303
$V_{40}Al_{60}$	1810	1.190±0.08	-4.879±0.64	1.194
$V_{30}Al_{70}$	1663	1.048±0.07	-5.218±0.68	0.976
$V_{25}Al_{75}$	1548	0.939±0.04	-4.517±0.58	0.824
$V_{20}Al_{80}$	1548	0.911±0.04	-4.874±0.63	0.787
$V_{10}Al_{90}$	1460	0.888±0.03	-4.735±0.62	0.726
Al	933	0.916±0.04	-2.223±0.59	0.723

Table 4: Parameters γ_L, γ_T and $\gamma(1800\ K)$ obtained for the pure elements Al and V in this work compared to literature data obtained with different measurement techniques. The method abbreviations are: EML = electromagnetic levitation, L = Literature Review, SD = sessile drop, ESL = electrostatic levitation, BP = bubble pressure, PD = pendant drop.

Composition	$\gamma_L[\mathrm{Nm}^{-1}]$	$\gamma_T[10^{-4}\mathrm{Nm}^{-1}K^{-1}]$	$\gamma(1800\ K)[\mathrm{Nm}^{-1}]$	Reference	Method
Al	0.916±0.04	-2.22±0.59	0.723	This work	EML
Al	0.866±0.03	-1.46±0.4	0.739	[34]	EML
Al	0.914	-3.5	0.611	[48]	L
Al	0.930	-1.46	0.803	[49]	SD
Al	0.825	-0.5	0.782	[49]	BP
V	1.934±0.07	-3.51±0.66	2.069	This work	EML
V	1.935±0.06	-2.7	2.038	[46]	ESL
V	1.950	-	-	[50]	PD
V	1.940±0.07	-3.29±0.70	2.066	[14]	EML

Table 5: Redlich-Kister parameters ${}^{0}L_{Al,V}(T)$ and ${}^{1}L_{Al,V}(T)$ [24] and the binary interaction parameter ${}^{0}V$ used for the model calculations in Eq. (4) and Eq. (10).

Parameter	Value	Unit
${}^{0}L_{Al,V}(T)$	$-57725 + 9 * \mathrm{T}$	$J\ mol^{-1}$
${}^{1}L_{Al,V}(T)$	$-18000 + 8 * \mathrm{T}$	$J\ mol^{-1}$
${}^{0}V$	-5.55	$cm^{3}mol^{-1}$

Figures

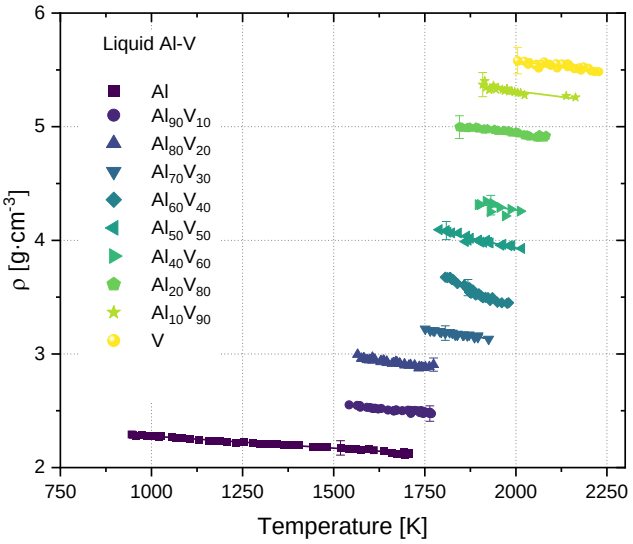

Figure 1: Density versus temperature for all investigated samples in the Al-V system. Linear fits following Eq. 1 are also included. The density decreases linearly with increasing temperature for all alloys. The density for the alloys lies between the density for the pure elements. The data is displayed without error bars for clarity reasons. The usual experimental error is ±1% as explained under II. B.

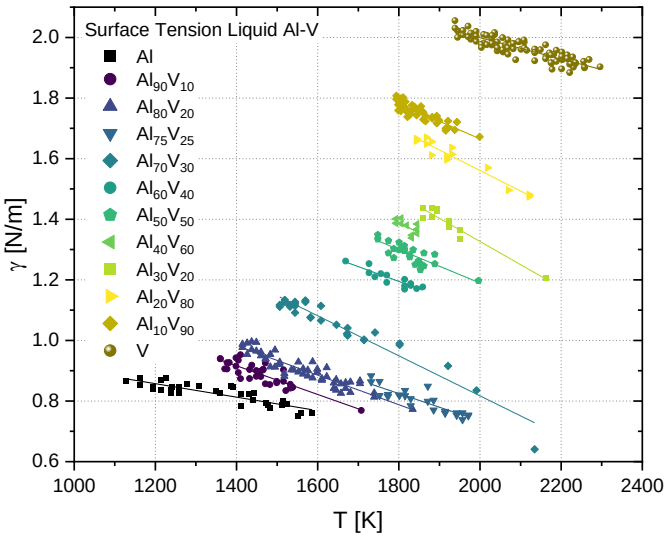

Figure 2: Surface tension versus temperature of all investigated alloys in the Al-V system. Surface tension decreases linearly with increasing temperature for all investigated samples. Linear fits according to Eq. 5 are included for every measurement as solid lines. Error bars have been left out for clarity reasons. As explained in II C. the experimental error is ±5%.

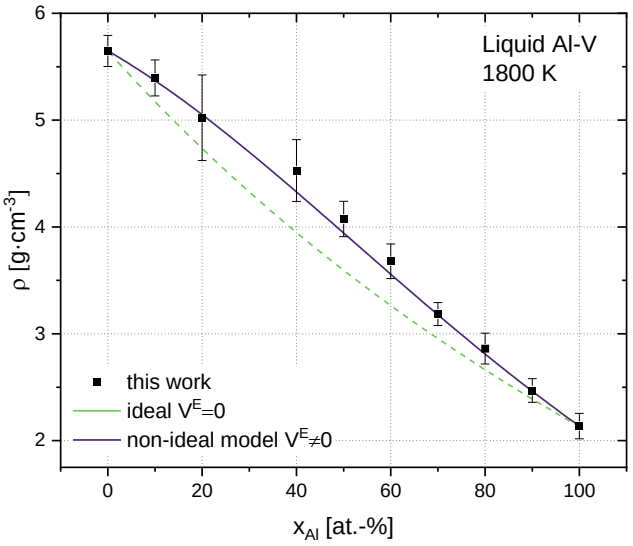

Figure 3:Density at the reference temperature 1800 K versus the mole fractionof aluminum. Fits for the ideal solution (dotted line) and the regular solution (solid line) are also included. The density decreases nearly linearly with increasing aluminum content. The experimental error was calculated using Eq. 21.

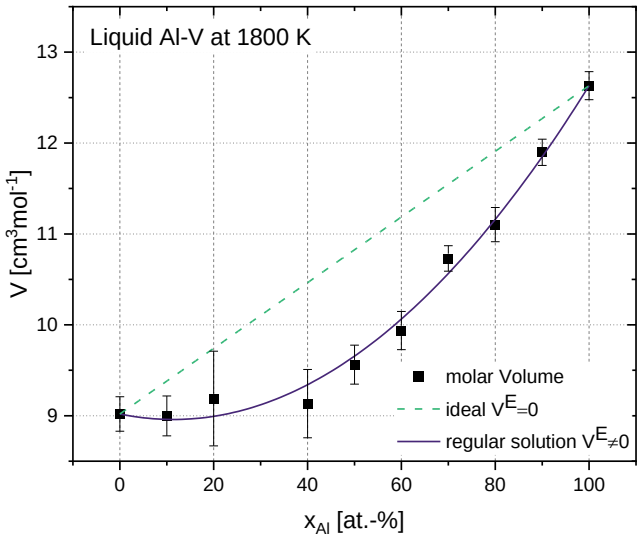

Figure 4: Molar Volume at 1800 K versus the aluminum mole fraction. Fits for the ideal (dashed line) and regular solution (solid line) are also included following Eq. 2. The molar volume increases with increasing aluminum content, but does not follow the linear behavior of the ideal solution. The experimental error was calculated using an analogous expression to equation 19.

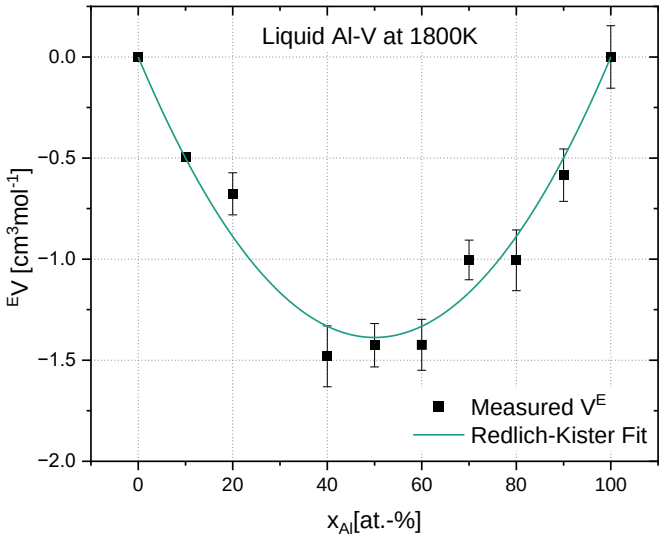

Figure 5: Excess volume versus the bulk mole fraction aluminum. The fit described by Eq. 4 is also included as a solid line. The resulting fitting parameter ^{0}V *can be found in table 5. The error results from the experimental error of V corresponding to error propagation.*

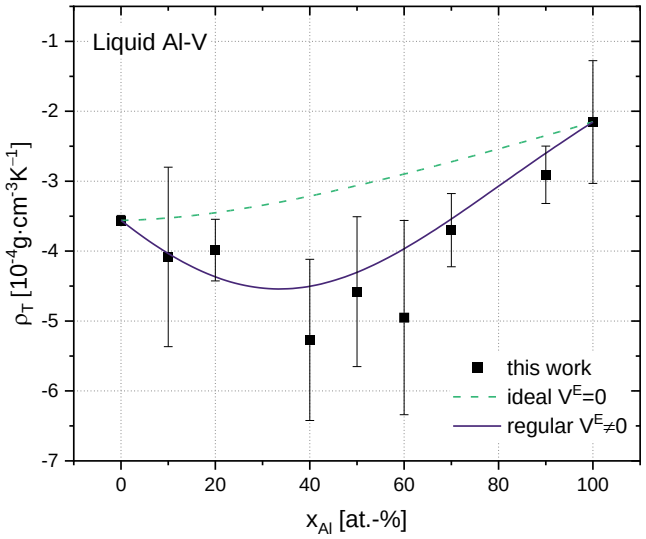

Figure 6: Temperature coefficient of liquid Al-V versus the bulk aluminum concentration. The dashed line represents the calculated volume for an ideal solution, the solid line the calculations for a regular solution. The error is adopted from the linear fits in Fig. 1.

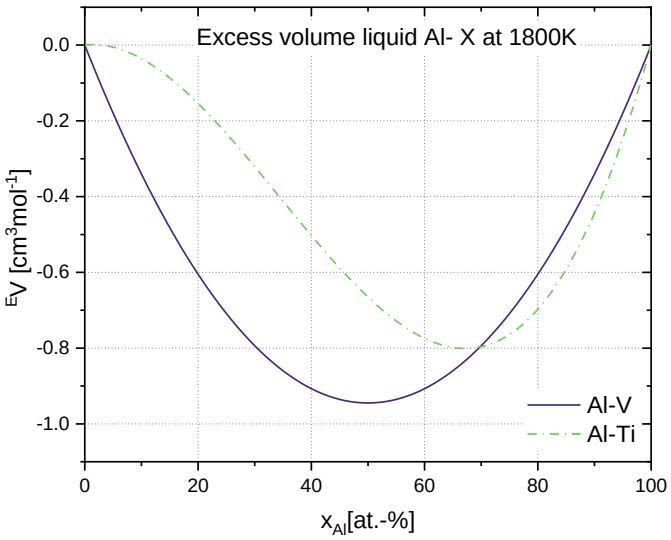

Figure 7: Comparison of the excess volume versus the aluminum mole fraction of the liquid Al-V and liquid Al-Ti system at 1800K. The data for Al-Ti was taken from Ref. [51].

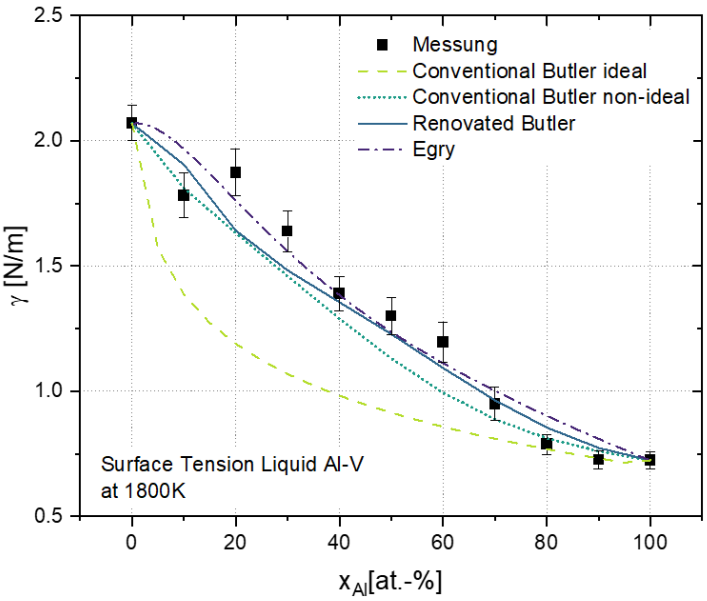

Figure 8: Surface tension of liquid Al-V at 1800K as a function of the aluminum mole fraction. Calculations for the Conventional Butler model of the ideal mixture (Eq. 12) is included as a dashed line and for the regular solution (Eq. 13) as a dotted line. The dash-dotted and solid line represent predictions made by the Egry model (Eq. 17) and the Renovated Butler model for the regular solution (Eq. 10) respectively. The experimental error has been estimated in accordance with [32] to be ±5%.

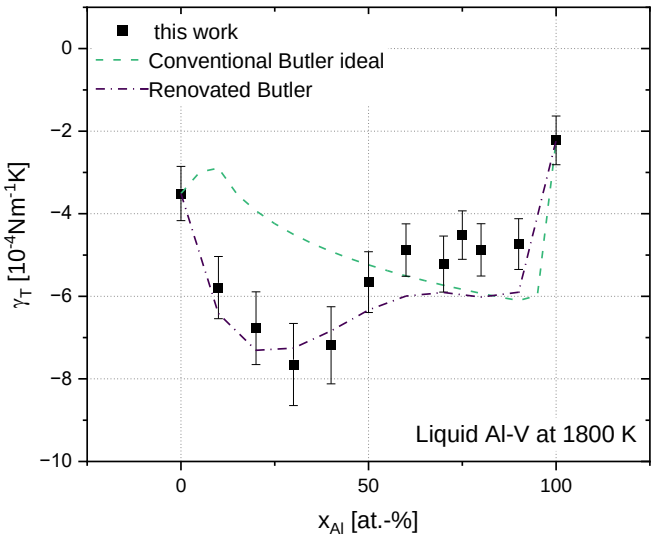

Figure 9: Measured temperature coefficients at 1800K for the linear fits in Fig. 2 according to Eq. 5 versus the mole fraction of aluminum. The coefficients calculated for an ideal solution according to the Conventional Butler model (Eq. 15) are included as dashed line and as dashed-dotted line for the regular solution following the Renovated Butler model (Eq. 10).

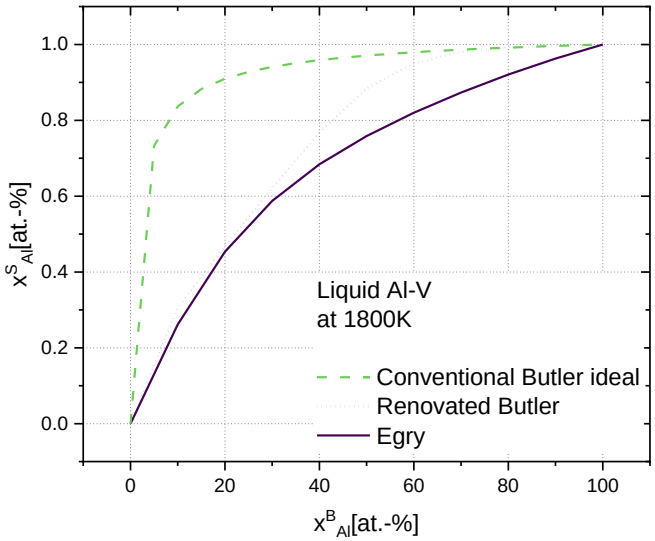

Figure 10: Surface composition of the liquid Al-V system at 1800K as a function of the aluminum bulk mole fraction. Data for the ideal Conventional (Eq.16) and Renovated Butler model (Eq. 10), as well as data for the Egry model (Eq. 17) are presented.

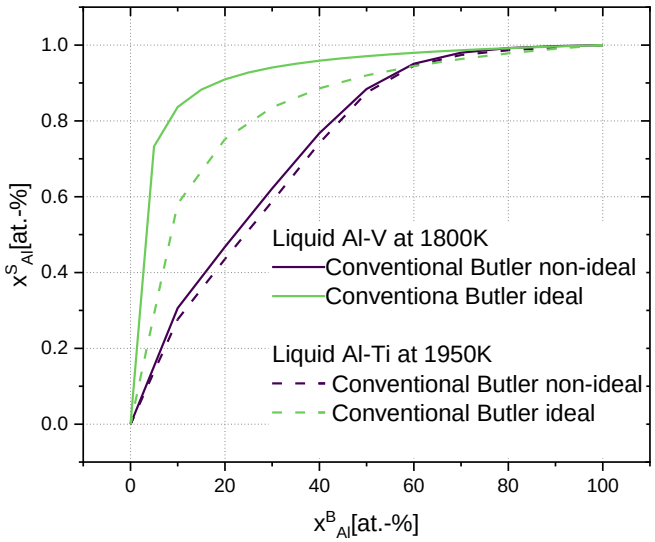

Figure 11: Surface composition of the Al-V (solid lines) system and the Al-Ti (dashed lines) system at 1800K as a function of the bulk mole fraction of aluminum. The composition has been calculated in accordance with the ideal and regular Butler model for both alloy systems.

VI. References

[1] C. Veiga, J. Davim and A. Loureiro, "Properties and Applications of Titanium Alloys: A Brief History," *Rev. Adv. Mater. Sci.*, no. 32, pp. 14-34, 2012.

[2] P. J. Bania, "Beta Titanium Alloys and Their Role in the Titanium Industry," *JOM*, no. 49, pp. 16-19, 1994.

[3] M. Peters, C. H. W. J. Kumpfert and C. Leyens, "Titanium Alloys for Aerospace Applications," *Advanced Engineering Materials*, no. 6, pp. 419-427, 2003.

[4] M. Niinomi, "Mechanical properties of biomedical titanium alloys," *Materials Science and Engineering*, no. 243, pp. 231-236, 1998.

[5] J. Wu, S. Zheng and Z. Li, "Thermal stability and its effects on the mechanical properties of rapidly solidified Al-Ti alloys," *Materials Science and Engineering*, no. 289, pp. 246-254, 2000.

[6] O. Ivasishin, P. Markovsky, S. Semiatin and C. Ward, "Aging response of coarse- and fine-grained beta titanium alloys," *Materials Science and Engineering A*, no. 405, pp. 296-305, 2005.

[7] M. Khan, R. Williams and D. Williams, "In-vitro corrosion and wear of titanium alloys in the biological environment," *Biomaterials*, no. 17, pp. 2117-2126, 1996.

[8] M. A.-H. Gepreel and M. Niinomi, "Biocompatibility of Ti-alloys for long-term implantation," *Journal of the machanical behavior of biomedical materials*, no. 20, pp. 407-418, 2013.

[9] G. Lütjering and J. Williams, Titanium, Berlin: Springer, 2007.

[10] J. J. Wessing and J. Brillo, "Density, Molar Volume, and Surface Tension of Liquid Al-Ti," *The Minerals, Metals & Materials Society and ASM International*, vol. 48, pp. 898-882, 2016.

[11] J. Brillo, J. J. Wessing, H. Kobatake and H. Fukuyama, "Normal spectral emissivity of liquid Al-Ti binary alloys," *High Temperatures-High Pressures*, vol. 48, pp. 423-438, 2019.

[12] J. Brillo, J. J. Wessing, H. Kobatake and H. Fukuyama, "Molar heat capacity of liquid Ti, Al20Ti80 and Al50Ti50 measured in electromagnetic levitation," *High Temperatures-High Pressures*, pp. 1-20, 2021.

[13] B. Reiplinger and J. Brillo, "Density and excess volume of the liquid Ti–V system measured in electromagnetic levitation," *Journal of Material Science*, pp. 1-11, 2022.

[14] B. Reiplinger, Y. Plevachuk and J. Brillo, "Surface tension of liquid Ti, V and their binary alloys measured by electromagnetic levitation," *Journal of Materials Science*, p. 21828–21840, 2022.

[15] Z. Cai, T. Shafer, W. Ikuya, M. E. Nunn and T. Okabe, "Electrochemical characterization of cast titanium alloys," *Biomaterials*, pp. 213-218, 2003.

[16] M. Taira, J. Moser and E. Greener, "Studies of Ti alloys for dental castings," *Dental Materials,* pp. 45-50, 1989.

[17] B. Baufeld, O. v. d. Biest and R. Gault, "Additive manufacturing of Ti–6Al–4V components by shaped metal deposition: Microstructure and mechanical properties," *Materials and Design,* vol. 31, pp. 106-111, 2009.

[18] S. Liu and Y. C. Shin, "Additive manufacturing of Ti6Al4V alloy: A review," *Materials and Design,* vol. 164, pp. 107552-(1-23), 2019.

[19] L.-C. Zhang, Y. Liu, S. Li and a. Y. Hao, "Additive Manufacturing of Titanium Alloys by Electron beam melting: a review," *Advanced Engineering Materials,* vol. 20, pp. 1700842-(1-16), 2018.

[20] J. Brillo, G. Lohofer, F. Schmidt-Hohagen, S. Schneider and I. Egry, "Thermophysical property measurements of liquid metals by electromagnetic levitation," *International Journal of Materials and Product Technology,* vol. 26, pp. 247-73, 2006.

[21] I. Egry, A. Diefenbach, W. Dreier and J. Piller, "Containerless Processing in Space Thermophysical Property Measurements using Electromagnetic Levitation," *International Journal of Thermophysics,* vol. 22, p. 569–578, 2001.

[22] J. Brillo, Thermophysical properties of multicomponent liquid alloys, Berlin/Boston: Walter de Gruyter GmbH, 2016.

[23] G. Kaptay, "Partial Surface Tension of Components of a Solution," *Langmuir,* no. 31, p. 5796–5804, 2015.

[24] A. Kroupa, M. Mazalová and K. Richter, "The reassessment of the Al-V system and new assessment of the Al-Si-V system," *CALPHAD: Computer Coupling of Phase Diagrams and Thermochemistry,* no. 59, pp. 47-60, 2017.

[25] G. Kaptay, "An improved derivation of the Butler equations for surface tension of solutions," *Langmuir,* no. 33, p. 10987–10992, 2019.

[26] T. P. Hoar and D. A. Melford, "The surface tension of binary liquid mixtures: lead + tin and lead + indium alloys," *Transactions of the Faraday Society,* no. 53, pp. 315-326, 1957.

[27] I. Egry, "Surface tension of compound forming liquid binary alloys: A simple model," *Journal of Material Science,* no. 39, pp. 6365-6366, 2004.

[28] J. Brillo and I. Egry, "Density of Multicomponent Melts Measured by Electromagnetic Levitation," *Japanese Journal of Applied Physics,* vol. 50, pp. 11RD02-(1-4), 2011.

[29] J. L. Margrave, S. Krishnan, G. P. Hansen and R. H. Hauge, "Spectral emissivities and optical properties of electromagnetically levitated liquid metals as functions of temperature and wavelength," *High temperature science,* vol. 29, pp. 17-52, 1990.

[30] H. Okamoto, "Al-V (Aluminum-Vanadium)," *Journal of Phase Equilibria and Diffusion,* no. 33, 2012.

[31] S. Sauerland, K. Eckler and I. Egry, "High-precision surface tension measurements on levitated aspherical liquid nickel droplets by digital image processing," *Journal of Materials Science Letters,* no. 11, p. pages 330–333.

[32] B. Reiplinger and J. B. Y. Plevachuk, "Experimental study of density, molar volume and surface tension of the liquid Ti-V system measured in electromagnetic levitation," *High Temperatures - High Pressures,* vol. 52, no. 2, pp. 175-190, 2023.

[33] S. Amore, J. Brillo and I. Egry, "Experimental measurment of surface tension of of Cu-Ti liquid alloys," *High Temperatures - High Pressures,* no. 40, pp. 225-235, 2011.

[34] J. Brillo and G. Kolland, "Surface tension of liquid Al-Au binary alloys," *J. Mater. Sci.,* 2016.

[35] J. Brillo, G. Lauletta, L. Vaianella, E. Arato, D. Giuranno, R. Novakovic and E. Ricci, "Surface tension of liquid Ag-Cu binary alloys," *ISIJ International,* vol. 54, pp. 2115-2119, 2014.

[36] L. Soldi, A. Quaini, S. Gosse, J. Brillo and M. Roskosz, "Thermodynamic and thermophysical properties of Cu-Si liquid alloys," *High Temperatures - High Pressures,* vol. 49, pp. 155-171, 2020.

[37] H. Kobatake and J. Brillo, "Density and viscosity of ternary Cr–Fe–Ni liquid alloys," *Journal of Materials Science,* vol. 48, p. 6818–6824, 2013.

[38] D. L. Cummings and D. A. Blackburn, "Oscillations of magnetically levitated aspherical droplets," *Journal of Fluid Mechanics,* no. 224, pp. 395-416, 1991.

[39] E. S. Levin, D. G. Ayushina and V. P. Geld, "Density and surface-energy polytherms of liquid (molten) aluminum," *High Temperature 6,* no. 3, p. 416, 1968.

[40] T. Saito, Y. Shiraishi and Y. Sakuma, "Density Measurement of Molten Metals by Levitation Technique at Temperatures between 1800°C and 2200°C," *Transactions of the Iron and Steel Institute of Japan,* no. 2, pp. 118-126, 1969.

[41] Y. Plevachuk, I. Egry, J. Brillo, D. Holland-Moritz and I. Kaban, "Density and atomic volume in liquid Al–Fe and Al–Ni binary alloys," *International Journal of Materials Research,* no. 98, pp. 107-1011, 2013.

[42] J. Brillo, I. Egry and J. Westphal, "Density and thermal expansion of liquid binary Al – Ag and Al – Cu alloys," *International Journal of Materials Research,* vol. 2, no. 99, pp. 162-167, 2013.

[43] J. Brillo, M. Watanabe and H. Fukuyama, "Relation between excess volume, excess free energy and isothermal compressibility in liquid alloys," *Journal of Molecular Liquids,* vol. 326, pp. 114395 1-35, 2021.

[44] B. Lindahl, X. Liu, Z. Liu and M. Selleby, "A thermodynamic re-assessment of Al–V toward an assessment of the ternary Al–Ti–V system," *Calphad,* no. 51, pp. 75-88, 2015.

[45] M. J. Assael and K. Kakosimos, "Reference Data for the Density and Viscosity of Liquid Aluminum and Liquid Iron," *Journal of Physical and Chemical Reference Data,* no. 35, pp. 285-300, 2006.

[46] J. T. Okada, T. Ishikawa, Y. Watanabe and P.-F. Paradis, "Surface tension and viscosity of molten vanadium measured with an electrostatic levitation furnace," *J. Chem. Thermodynamics,* no. 42, pp. 856-859, 2010.

[47] D. J. Steinberg, "A Simple Relationship Between the Temperature Dependence of the Density of Liquid Metals and Their Boiling Temperatures," *METALLURGICAL TRANSACTIONS,* pp. 1341-1344, 1974.

[48] T. Tanaka and T.Iida, "Application of a thermodynamic database to the calculation of surface tension for iron-base liquid alloys," *Steel Research International,* no. 65, pp. 21-28, 1994.

[49] B. J. Keene, "Review of data for the surface tension of pure metals," *International Materials Reviews,* vol. 4, no. 38, pp. 157-192, 1993.

[50] B. C. Allen, "THE SURFACE TENSION OF LIQUID TRANSITION METALS AT THEIR MELTING POINTS," *Trans. AIME,* no. 227, p. 1175, 1963.

[51] J. J. Wessing, "Thermophysical properties of liquid Al-Ti alloys under the influence of oxygen," *Doctoral dissertation, RWTH Aachen Chair for Foundry Science and Foundry Institute,* 2018.

[52] T. Ishikawa, P.-F. Paradis, T. Itami and S. Yoda, "Non-contact thermophysical property measurements of refractory metals using an electrostatic levitator," *Measurement Science and Technology,* vol. 16, pp. 443-451, 2005.

[53] M. Qian, W. Xu, M. Brandt and H. Tang, "Additive manufacturing and postprocessing of Ti-6Al-4V for superior mechanical properties," *MRS Bulletin,* vol. 41, pp. 775-784, 2016.

[54] I. Egry, A. Diefenbach, W. Dreier and J. Piller, "Containerless Processing in Space—Thermophysical Property Measurements Using Electromagnetic Levitation," *International Journal of Thermophysics,* p. 569–578, 2001.

[55] J. A. V. Butler, "The thermodynamics of the surfaces of solutions," *Proceedings of the Royal Society A,* no. 827, pp. 348-376, 1932.

[56] G. Kaptay, "A unified model for the cohesive enthalpy, critical temperature, surface tension and thermal volume thermal expansion coefficient of liquid metals of bcc, fcc, and hcp crystals," *Mater. Sci. Eng. A,* vol. 495, pp. 19-26, 2008.

[57] T. Tanaka, K. Hack, T. Iida and S. Hara, "Application of thermodynamic databases to the evaluation of surface tensions of molten alloys, salt mixtures and oxide mixtures," *Zeitschrift für Metallkunde,* no. 87, pp. 380-389.

[58] J. Brillo, T. Schumacher and K. Kajikawa, "Density of Liquid Ni-Ti and a New Optical Method for its Determination," *The Minerals, Metals & Materials Society and ASM International,* vol. 50, pp. 924-935, 2018.